SCANNING VOL. 38, 113–120 (2016)

Improving Dimensional Measurement From Noisy Atomic Force Microscopy Images by Non-Local Means Filtering

Yuhang Chen

Department of Precision Machinery and Precision Instrumentation, University of Science and Technology of China, Hefei, Anhui, P. R. China

Summary: Quantitative evaluation of dimensional parameters from noisy atomic force microscopy (AFM) images was investigated. Non-local means (NLM) denoising was adopted to reduce noise and maintain fine image structures. Major tuning parameters in NLM filtering, such as the patch size and the window size, were optimized on simulated surface structures. The ability of dimensional evaluation from noisy data was demonstrated to be improved by almost 15 times. Finally, NLM filtering with optimal settings was applied on experimental AFM images, which were scanned on a patterned few-layer graphene specimen. Evaluations of the step height and the pattern size were verified to be much more accurate and robust. Such a data processing method can enhance the AFM dimensional measurements, particularly when the noise-level is reached. SCANNING 38:113–120, 2016. © 2015 Wiley Periodicals, Inc

Key words: dimensional measurement, non-local means filtering, atomic force microscopy, surface nanometrology

Introduction

Devices with critical dimensions at the micro-and-nano scale have attracted many attentions owing to their superior functional performances (Carlson *et al.*,2012). In various characterizations, the measurement and evaluation of dimensional parameters with ultrahigh precision are of fundamental importance. Toward this purpose, many techniques have been developed (Hansen *et al.*, 2006). Among them, atomic force microscopy (AFM) is one of the most powerful and flexible tools. AFM and its analogs have remarkable capability of two-and-a-half-dimensional measurements of almost all kinds of samples, and they have obtained tremendous applications in surface dimensional nanometrology (Dai *et al.*, 2006).

Under the same noise level, the measured data can gradually emerge relatively low signal-to-noise ratio along with the decrease of the critical dimensions of the sample structures. Consequently, the quantitative determination of geometrical parameters may become rather difficult. For instance, few-layer graphene (FLG) based devices with the thickness ranging from mono-atomic layer to several layers have appeared as a leading-edge research area. Of such devices, many interesting physical properties depend closely on the number of layers (Dimiev *et al.*, 2011). However, determination of the graphene layers or the equivalent step heights by AFM has a large uncertainty as reported in literature (Nemes-Incze *et al.*, 2008). The possible reasons may rely on the improper imaging parameters, the substrate roughness (Lui *et al.*, 2009) and the low signal-to-noise ratio in data acquisition. Reliable analysis methods are still somewhat lacking (Baumann *et al.*, 2014).

In addition, we should note that though the measurement resolution of AFM reaches sub-nanometer scale, the effective dimensions of common calibration standards are mostly much larger. The existence of such a gap may lead to incomplete characterization of the microscope performance. To overcome this barrier, reference structures with reduced dimensions and associated analysis methods are highly demanded. Therefore, calibration standards, for instance silicon crystals with mono-atomic steps, have been proposed to enhance AFM's usefulness as a metrology tool (Orji *et al.*, 2004). When measuring all these ultra-thin films or super-small-scale structures with an ordinary AFM, we frequently encounter the practical situations that the measurands are rather close to the noise level. As a result, the quantitative dimensional evaluation from the

Contract grant sponsor: National Natural Science Foundation of China; Contract grant number: 51275503.

Address for reprints: Yuhang Chen, Department of Precision Machinery and Precision Instrumentation, University of Science and Technology of China, Hefei 230026, Anhui, P. R. China
E-mail: chenyh@ustc.edu.cn

Received 20 April 2015; Accepted with revision 4 June 2015

DOI: 10.1002/sca.21246
Published online 21 July 2015 in Wiley Online Library (wileyonlinelibrary.com).

noisy data becomes one of the major challenges (Edwards, '97).

For AFM data denoising, conventional Gaussian smoothing is quite popular owing to its simplicity and robustness (Liu *et al.*, 2011). However, Gaussian smoothing tends to blur certain sharp structures simultaneously because a local average kernel is applied. This over-smoothing effect is unacceptable for quantitative dimensional evaluation. The ideal way is to keep all the fine geometries while remove the noise completely. Non-local means (NLM) filtering is probably one of the most effective approaches that can meet this challenge. After the first introduction of such a data adaptive denoising method (Buades *et al.*, 2005), several modifications have been made to improve its performances and to implement it in various research fields (Wang *et al.*, 2012; Wu *et al.*, 2013). However, NLM algorithms are usually employed to enhance the image quality (Manjón *et al.*, 2008). In dimensional measurements, we concern more about the quantitative values and their accuracy. Until now, a systematic investigation on applying NLM for surface metrology remains lacking. Furthermore, parameters for tuning the NLM performances should be optimized accordingly (Salmon, 2010).

Concerning all these situations, here we implemented NLM in AFM data processing to improve dimensional measurements. Especially, the case of measuring sample dimensions, which are comparable with the noise level, was addressed. First, topography datasets with precisely assigned geometrical characteristics and variable noise strengths were numerically generated. Then, the main tuning parameters in NLM algorithms were optimized for better accuracy. Last, using the optimal parameters, the capability of NLM filtering was verified on experimental AFM data, which were acquired on patterned FLG structures.

Methods

Simulation Data Generation

As a prototype of sample structures for evaluating the NLM performances, a stepped surface is numerically generated with the random roughness simulating the noise distribution. The lower half surface has a mean height h_l, and a height standard deviation σ. The upper half surface has a mean height h_u and the same standard deviation σ. For both half surfaces, Gaussian height distributions are assumed and surface autocorrelation functions are in the form of,

$$c(x,y) = \sigma^2 \exp\left\{-2.3\left[\left(\frac{x}{\tau_x}\right)^2 + \left(\frac{y}{\tau_y}\right)^2\right]\right\} \quad (1)$$

where τ_x and τ_y are the autocorrelation lengths in x and y directions, respectively. The factor 2.3 means that the autocorrelation length here is taken at the 10% decay. A general relation $\tau_x = \tau_y$ is applied, that is, the noise is spatially homogenous in the simulations (Chen *et al.*, 2013). Considering the fact that the measurement noise should not be too much spatially correlated, the autocorrelation length is assigned with a small magnitude, for instance, 1 or 2 pixels.

The roughness surfaces were generated using the two-dimensional (2D) digital filter method (Liu *et al.*, 2012). The topographic data were stored in a 2D matrix with 128×256 pixels as depicted in Figure 1a. We applied a slight height difference between the upper half surface and the lower half surface, and $h_s = h_u - h_l$ was set as 0.5 arbitrary units. The standard deviation σ was normalized to 1 unit and the autocorrelation length was 2 pixels. From the height histogram (Fig. 1b), we can find that the step signal is actually immersed in the noise and only a unique near-Gaussian distribution peak is observable. Therefore, the existence of the surface step cannot be clearly figured out either from the height histogram or by the step function fitting. After smoothing, still only one distribution peak presents with the mean central height of 0.24 units, which is the same as the one deduced from the raw surface data. Therefore, the assigned step of 0.5 units remains undistinguishable and the main effect is that the standard deviation is reduced from 1.23 units to 0.73 units. Here, a normalized 5×5 low-pass Gaussian filter was applied

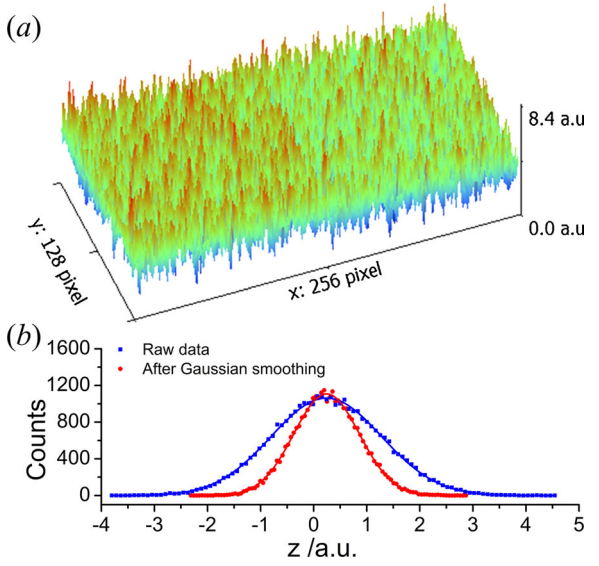

Fig 1. Typical simulated noisy surface for exploring the effect of NLM filtering in dimensional measurement. (a) Three-dimensional view of the generated surface. The upper half (left part) surface and the lower half (right part) surface have a height difference of 0.5 units. (b) Height distribution histograms of the raw surface and the Gaussian-smoothed surface. From both histograms, the presence of a step is undistinguishable.

with the kernel matrix as,

$$\mathbf{G} = \begin{bmatrix} 0.0030 & 0.0133 & 0.0219 & 0.0133 & 0.0030 \\ 0.0133 & 0.0596 & 0.0983 & 0.0596 & 0.0133 \\ 0.0219 & 0.0983 & 0.1621 & 0.0983 & 0.0219 \\ 0.0133 & 0.0596 & 0.0983 & 0.0596 & 0.0133 \\ 0.0030 & 0.0133 & 0.0219 & 0.0133 & 0.0030 \end{bmatrix} \tag{2}$$

By carefully adjusting the filter kernel, the residual noise might be further removed. However, real surface structures including the step edges will be blurred simultaneously. When the step height is comparable with the noise level, Gaussian smoothing is not very effective. Thus, we have to consider other methods and NLM filtering is an appropriate approach. Generally, it recovers the signal at each sampling point by employing a weighted average, which is a robust similarity measure taking the neighboring pixels into account (Buades *et al.*, 2005). NLM filtering has the capability of removing the noise efficiently while preserving fine features in the original image (Wang *et al.*, 2012).

Non-Local Means Denoising

In this section, we briefly review the NLM processing procedures. Detailed principles can be found in the references (Buades *et al.*, 2005; Wu *et al.*, 2013). A scanned AFM image can be described as $\mathbf{z} = \{z_i\}_{i \in \boldsymbol{I}}$, which is defined on a 2D spatial domain $\mathbf{I}$. The dataset $\mathbf{z}$ contains the true topography, certain artifacts and the noise. Separations of specified image artifacts, such as those induced by scanner nonlinearity (Jin and Bruck, 2005) and transient responses (Chen and Huang, 2010), need a thorough analysis of the corresponding error sources and a subsequent proper modeling. For simplicity, we neglect these distortions and only the random noise is considered, that is,

$$z_i = \widehat{z}_i + n_i \tag{3}$$

where $\widehat{z}_i$ is the expected true height, and n_i is the Gaussian noise with a zero mean and an unknown variance σ^2.

In the NLM algorithms, the real surface height at each sampling point is estimated by applying a weighted sum of the noisy data within a search window $\mathbf{W}$,

$$\widehat{z}_i = \sum_{j \in \mathbf{W}} \frac{w_{i,j}}{w_i} z_j \tag{4}$$

In the above equation, the weight function $w_{i,j}$ is (Buades *et al.*, 2005),

$$w_{i,j} = \exp\left[-\sum_{k \in \mathbf{P}} \frac{(z_{i+k} - z_{j+k})^2}{g^2} \right] \tag{5}$$

Here, g is a parameter that regulates the smoothing strength via controlling the decay of the exponential function. As shown in the equation, the NLM approach takes not only the characteristic in a local domain but also the geometrical configuration in a whole neighborhood into account by using a proper patch $\mathbf{P}$. The summation of all the weights, which behaves as a normalizing constant in Equation 4, is calculated by,

$$w_i = \sum_{j \in \mathbf{W}} w_{i,j} \tag{6}$$

In the following, we adopted a modified weight kernel as proposed by Wu and his cooperators (Wu *et al.*, 2013). First, the difference between the two patches, which are squared neighborhoods centering at z_i and z_j, can be evaluated,

$$D_{i,j} = \sum_{k \in \mathbf{P}} \frac{(z_{i+k} - z_{j+k})^2}{2\sigma^2} \tag{7}$$

Here, $D_{i,j}$ is interpreted as the standard χ^2 test to measure patch similarity (Thacker *et al.*, 2010). Comparing Equations 5 and 7, it is obvious that they are somewhat similar, but the measure of the patch similarity in the latter one is statistically rigorous. Therefore, instead of using the exponential decay function, a probabilistic weight can be adopted, which is deduced as (Wu *et al.*, 2013),

$$w_{i,j} = \frac{(D_{i,j}/\gamma_{i,j})^{\eta_{i,j}/2-1} \exp(-D_{i,j}/2\gamma_{i,j})}{2^{\eta_{i,j}/2}\Gamma(\eta_{i,j}/2)} \tag{8}$$

Here, Γ is the gamma function. Parameters $\gamma_{i,j}$ and $\eta_{i,j}$ are,

$$\gamma_{i,j} = \frac{\sum_{k,l \in \mathbf{P}} cov[d_{i+k,j+k}, d_{i+l,j+l}]}{2|\mathbf{P}|} \tag{9}$$

$$\eta_{i,j} = \frac{|\mathbf{P}|}{\gamma_{i,j}} \tag{10}$$

In above equations, $|\mathbf{P}|$ denotes the number of pixels in patch $\mathbf{P}$. And we have,

$$d_{i,j} = \frac{(z_i - z_j)^2}{2\sigma^2} \tag{11}$$

Combining Equations 8–11, the weight function can be calculated and the filtered image is finally obtained using Equation 4. The last critical issue is that the noise variance σ^2 is unknown and an estimated value has to be adopted,

$$D_{i,j} = \frac{\widehat{D}_{i,j}}{\rho^2} \quad (12)$$

Here, $\widehat{D}_{i,j}$ represents the patch similarity measure calculated using the estimated variance and ρ^2 is a tuning parameter.

Figure 2 shows typical NLM denoising results of the raw image presented in Figure 1. The existence of a step can be clearly found in both the filtered topography and its corresponding height histogram. In filtering, the patch size and the window size were 7×7 and 21×21, respectively. The tuning factor ρ^2 was 3 and an estimated $\hat{\sigma}$ of 0.59 units was used. From the histogram, the lower half surface locates at the zero-height position with a standard deviation of 0.14 units and the upper half surface centers at a mean height of 0.48 units with a standard deviation of 0.15 units. Then, the step height is determined to be 0.48 units, which is in a good agreement with the assigned 0.5 units. By implementing NLM filtering, the step height was reliably restored from the noisy data.

Results and Discussion

Parameters Optimization

From the above brief introduction of the probabilistic NLM, it is obvious that three main parameters can be adjusted, namely the patch size, the window size and the tuning factor ρ. As can be seen in Equation 12, the tuning factor is adopted to alter the estimated $\widehat{\sigma}$ to match the real standard deviation σ, which is prior unknown in practical situations. Along with the increase of σ, a larger patch and a larger search window are generally required to make the patch comparison robust and the noise removal capacity enhanced by finding more similar imaging pixels. On the other hand, the patch size should be small enough to preserve fine structures. It is therefore necessary to optimize these NLM parameters for applications in surface metrology.

Toward this purpose, we applied a series of calculations on a numerically designed surface similar to that presented in Figure 1. The main geometrical parameters are listed as autocorrelation length of 1 pixel, step height of 1 unit, and standard deviations of both the lower half surface and the upper half surface of 1 unit. Note that the height histogram of the original surface fails to provide clear evidence on the presence of a step. Figure 3 shows the results of optimizing the patch size. Here, we used the same window size of 15×15 and the tuning parameter ρ^2 of 1. The patch size was varied from 3×3 to 11×11. From the results, the determined step height first increases and then decreases with the increase of the patch size while the width of the height distribution peak behaves conversely. Under each set of NLM parameters, the step height can be precisely determined with the relative error ranging from -0.5% to -1.2%. In addition, the width of the distribution peak is the smaller the better for an accurate evaluation. Considering these requirements, a patch size within the range from 5×5 to 9×9 as covered in the shaded region is a better choice.

Figure 4 shows the optimization results of the window size. Here, the patch size was selected to be 5×5 and the tuning factor ρ^2 was set to 1 for each NLM processing. When the window size is varied from 7×7 to 25×25, the measured step height first approaches closer to the assigned value and then reaches a stable region. For the height distribution peak width, it decreases monotonously with the increase of the window size. It should be mentioned that the computational cost will also increase if a larger window is adopted. Thus, to make a compromise, a window size ranging from 13×13 to 23×23 as illustrated in the shaded region should be effective enough.

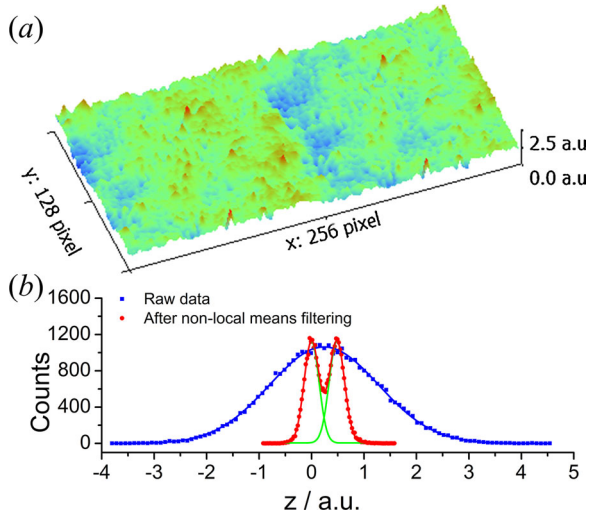

Fig 2. NLM filtering on the simulated surface. (a) Three-dimensional view of the filtered surface. (b) Comparisons of the height histograms of the raw surface and the filtered surface. The assigned step of 0.5 units is clearly visible after NLM filtering.

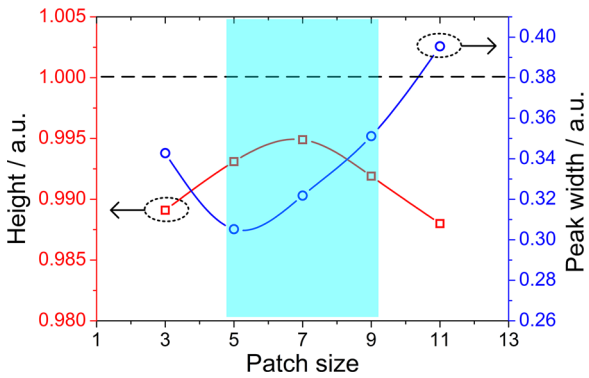

Fig 3. Optimization of the patch size in NLM filtering. Here, the adopted window size is 15×15 and the tuning factor ρ^2 is 1. The dashed line indicates the expected step height and the optimal range of the patch size is shaded.

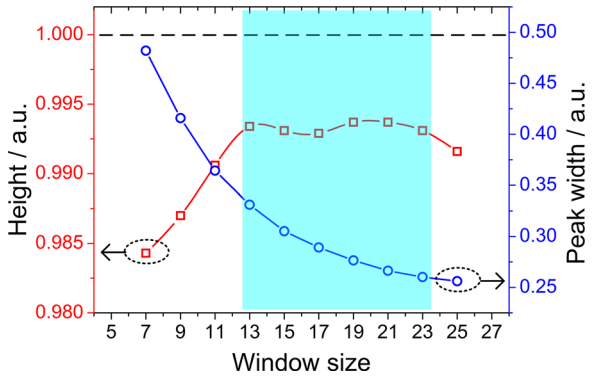

Fig 4. Optimization of the window size in NLM filtering. Here, the adopted patch size is 5×5 and the tuning factor ρ^2 is 1. The dashed line represents the expected step height and the optimal range of the window size is shaded.

The last parameter to be optimized is the tuning factor. We performed the analysis on two sets of surfaces. The first one was assigned with the autocorrelation length of 1 pixel and the other with the autocorrelation length of 2 pixels. All the other parameters were the same as those in the analyses corresponding to Figures 3 and 4. A patch size of 5×5 and a window size of 21×21 were applied, with both in the optimal regions. The evaluated step height and the height distribution peak width are presented in Figure 5. Note that they are respectively plotted as the mean value and the error bar. When the autocorrelation length of the spatial noise is 1 pixel, the suitable ρ^2 value falls in the range from 1.0 to 2.0. However, when the autocorrelation length increases to 2 pixels, the optimal range of parameter ρ^2 is from 2.5 to 3.5. That is to say, if the noise distribution is somewhat spatially correlated, the tuning factor ρ^2 has to be increased despite the fact that the noise variance σ^2 is the same.

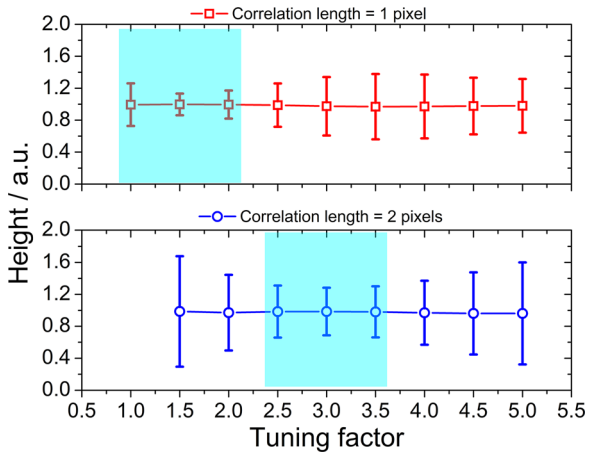

Fig 5. Optimization of the tuning factor ρ^2 in NLM filtering. Here, the patch size is 5×5 and the window size is 21×21. The optimal range of the tuning factor is shaded. If the noise is spatially correlated, the optimal tuning factor should increase accordingly.

Measurable Limit

To further explore the advantage of NLM processing, a rough estimation on the improvement of the measurable limit is carried out. A series of surfaces were simulated with the step height decreasing from 3.0 to 0.2 units. For each surface, the autocorrelation length was 1 pixel and the standard deviation of the surface height was 1 unit. Following previous optimizations, the patch size of 5×5, the window size of 21×21 and the tuning factor ρ^2 of 1.5 were selected. Figure 6 depicts the mean height positions together with the distribution peak widths of both the lower half surface and the upper half surface obtained from the filtered data. A step height of 0.2 units can be accurately measured under the noise variance σ^2 of 1 unit. However, the step becomes undistinguishable when the height further decreases to 0.1 units. The detection limit in this case is thus approximately 0.2 units.

For a simple analysis, the height distributions of the lower surface and the upper surface have the Gaussian form of,

$$y_l = A \exp\left(-\frac{z^2}{2\sigma^2}\right) \tag{13}$$

$$y_u = A \exp\left[-\frac{(z-h)^2}{2\sigma^2}\right] \tag{14}$$

Here, A is the amplitude of the maximum peak and h is the height difference as schematically illustrated in the inset of Figure 6. Using the Rayleigh criterion, the two peaks are unable to be separated, i.e. the step height is immeasurable when the minimum saddle value exceeds 81% of the maximum peak (Lentzen, 2008). The local minimum of $(y_l + y_u)$ locates at $z = h/2$,

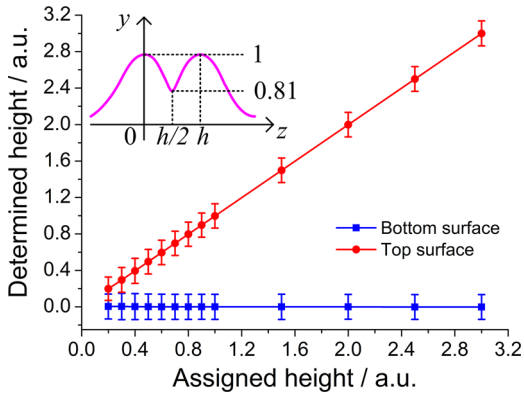

Fig 6. Detection limit of the step height after NLM filtering. The assigned height decreases from 3.0 units to 0.2 units. The mean heights and widths of distribution peaks of the upper half surface and the lower half surface are plotted. The inset schematically sketches the Rayleigh criterion in analyzing the step height by distribution histogram.

$$y_{\min} = 2A \exp\left(-\frac{h^2}{8\sigma^2}\right) \quad (15)$$

And the maximum locates at $z = 0$ or $z = h$,

$$y_{\max} = A\left[1 + \exp\left(-\frac{h^2}{2\sigma^2}\right)\right] \quad (16)$$

By solving the equation $y_{\min} = 0.81 y_{\max}$, the limit of the detectable height difference can be estimated by,

$$h_{lim} = 2.64\sigma \quad (17)$$

For the raw surface data, σ equals 1 unit and so the minimum detectable h_{lim} is 2.64 units. After NLM filtering with the optimized settings, we can usually reduce σ to a magnitude of 0.07 units. Then, the detectable step height limit h_{lim} is 0.18 units and this magnitude is in a close agreement with the numerical simulations presented in Figure 6. NLM improves the measurable limit up to 15 times, which is rather promising.

Applications on Experimental Images

As a further demonstration, we applied the NLM method on experimental AFM data. The sample structures were fabricated by anisotropic etching on a piece of graphene sheet, with a patterned array of holes as defects (Shi *et al.*, 2011). Figure 7a shows the raw image and the measured image quality is generally acceptable with clear hexagonal pattern. However, obvious noise presents in the topography, which can distort the dimensional measurement. The filtered image is depicted in Figure 7b. Here, the patch size of 7×7, the window size of 21×21 and the tuning parameter ρ^2 of 3 were selected within the optimal ranges. In fact, we have also tried other parameters in filtering (data not shown), and the above settings are among the best ones. Such results additionally demonstrate that the previous optimizations can provide a general guide on the selection of NLM parameters. From the smoothed image and the comparison of sectional profiles in Figure 7b and c, most noise is removed and no obvious distortions on the step edges occur. These characteristics of NLM smoothing prevail against many other methods.

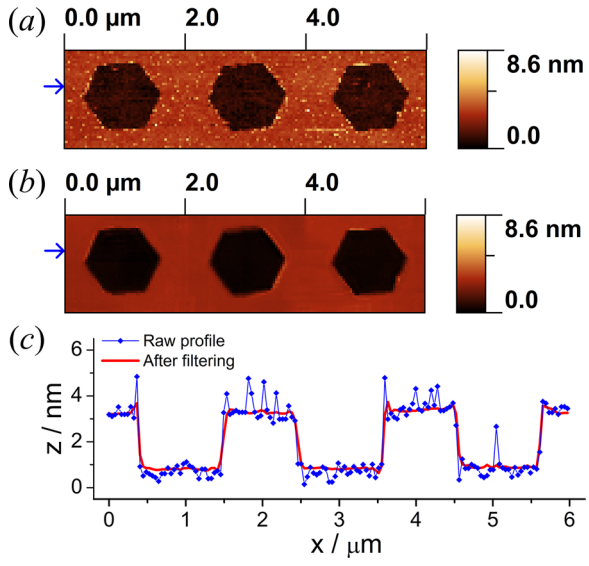

Fig 7. Application of NLM in processing practical AFM data. (a) Raw AFM image of a patterned few-layer graphene. (b) Filtered image. (c) Comparison of sectional profiles before and after filtering. The profiles are taken from the same position, as illustrated by two arrows in the topography images.

Figure 8 compares the height histograms of the topographic data with and without the NLM pre-processing. The step height determined from the original surface data is 2.37 nm, and the width of the height distribution peak is 0.49 nm. After filtering, they are 2.46 nm and 0.19 nm, respectively. The two step heights are in a close agreement, with a relative discrepancy of approximately 3.8%. Considering the interlayer distance in bulk graphite of 340 pm (Lui *et al.*, 2009), the steps contain approximately 7 graphene layers. In this case, the height signal is larger than the noise level satisfying $h > 2.64\sigma$ and therefore, it can be determined accurately even using the raw data.

The notable advantage of NLM filtering is that the filtered image shows almost binary features and undistorted original steep steps. We can easily extract the pattern boundaries for further enhanced evaluations of xy dimensions. Figure 9 illustrates the automatic determination of the lengths and the angles of the hexagon-like graphene patterns. The flowchart is sketched in Figure 9a. First, NLM filtering is performed on the raw data using the optimized tuning parameters. Such an operation usually leads to fairly clean image (see Figure 7b). Second, conventional edge detection and boundary tracing are applied. Owing to the superior image quality and almost binary height distribution of the filtered data, the edge detections are rather simple and robust. Third, the extracted

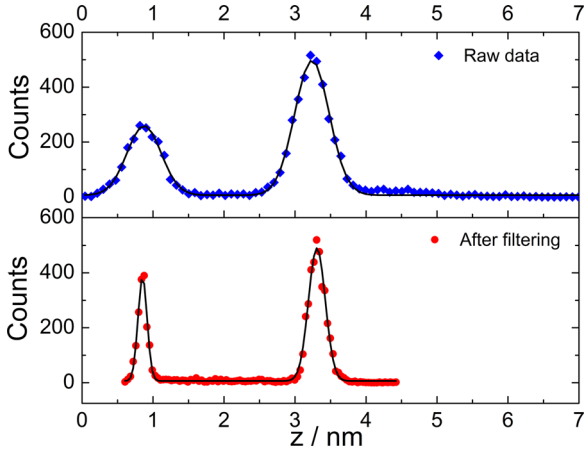

Fig 8. Histograms of height distributions before and after NLM filtering.

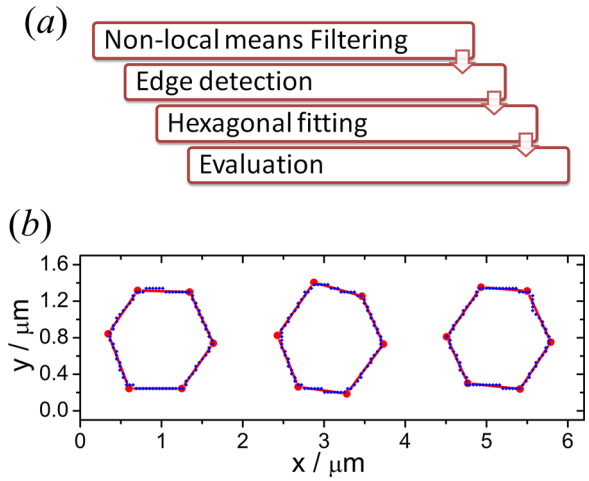

Fig 9. Evaluation of geometrical parameters of the graphene pattern. (a) Flowchart of the analysis procedure. (b) Extracted pattern boundaries (solid circles) and hexagonal fitting (straight lines). Red dots denote the fitted vertices of the near-hexagon pattern.

boundaries are linearly fitted as presented in Figure 9b. Last, the six fitted lines in each pattern are used to calculate the lengths and the angles. With such a procedure, the hexagon edge length is evaluated to be 633.43 ± 43.82 nm and the angle is 120.00 ± 5.16 degrees. Because the fluctuations in length and angle also contain AFM measurement errors, the fabrication errors should be even smaller than the determined ones, i.e. relative errors of 6.9% for the edge length and 4.3% for the angle. Two indications can be drawn from the results. First, NLM filtering can simultaneously improve the dimensional measurement in the *xy* plane. Second, the FLG shapes are nearly perfect uniform hexagons and the steps are an integer multiple of the single-layer thickness.

In addition to their applications in novel electronic devices (Shi *et al.*, 2011), the controllable and scalable geometrical patterns enable such nanostructures promising candidates for calibrating AFM at a smaller dimensional scale than conventional calibration standards. Using the nearly ideal hexagonal graphene patterns, it is hopeful to calibrate various behaviors of the microscopes, for example, scan orthogonality and thermal drift. However, toward these potential applications, further investigations on the stability of the FLG structures and the ultimate size limit of fabrication are necessary. Anyway, the NLM technique is capable of enhancing reliable dimensional evaluations under the conditions of noisy measurements and calibrations.

Conclusions

Quantitative dimensional evaluation from noisy data was investigated. With NLM denoising, noisy AFM images can be greatly smoothed while keeping fine surface structures undistorted. By systematic numerical investigations, the tuning parameters in NLM algorithms were optimized, including the patch size, the window size and the tuning factor. The optimizations were performed on a virtual surface step with random roughness simulating the noise distribution. Results demonstrated that a patch size ranging from 5×5 to 9×9 and a window size ranging from 13×13 to 23×23 can usually benefit more accurate image measurements. If the noise is somewhat spatially correlated, the NLM tuning factor should increase accordingly for effective noise elimination.

After parameters optimization of NLM filtering, the ability of dimensional evaluation from noisy data was demonstrated to be improved by almost 15 times. Finally, the method was applied on experimental AFM images of hexagonal FLG patterns. With the NLM image pre-processing, the evaluations of step height and pattern size were verified to be robust and accurate. Such a data analysis method can enhance the evaluation of structural dimensions, especially when they are close to the noise-level of microscopic measurements.

References

Baumann S, Rau IG, Loth S, Lutz CP, Heinrich AJ. 2014. Measuring the three-dimensional structure of ultrthin insulating films at the atomic scale. ACS Nano 8:1739–1744.

Buades A, Coll B, Morel JM. 2005. A non-local algorithm for image denoising. Proc. CVPR IEEE 2:60–65.

Carlson A, Bowen AM, Huang Y, Nuzzo RG, Rogers JA. 2012. Transfer printing techniques for materials assembly and micro/nanodevice fabrication. Adv Mater 24:5284–5318.

Chen Y, Huang W. 2010. Elimination of periodic damped artifacts in scanning probe microscopy images. Meas Sci Technol 21:045501.

Chen Y, Zhang X, Luo T, Liu X, Huang W. 2013. Fabrication and characterization of areal roughness specimens for applications in scanning probe microscopy. Meas Sci Technol 24:055402.

Dai G, Pohlenz F, Xu M, et al. 2006. Accurate and traceable measurement of nano- and microstructures. Meas Sci Technol 17:545–552.

Dimiev A, Kosynkin DV, Sinitskii A, et al. 2011. Layer-by-layer removal of graphene for device patterning. Science 331:1168–1172.

Edwards H. 1997. New method to estimate step heights in scanning-probe microscope images. Nanotechnology 8:6–9.

Hansen HN, Carneiro K, Haitjema H, De Chiffre L. 2006. Dimensional micro and nanometrology. Ann CIRP 55: 721–743.

Jin H, Bruck HA. 2005. A new method for characterizing nonlinearity in scanning probe microscopes using digital image correlation. Nanotechnology 16:1849–1855.

Lentzen M. 2008. Contrast transfer and resolution limits for sub-angstrom high-resolution transmission electron microscopy. Microsc Microanal 14:16–26.

Liu Q, Wang H, Liu J, Huang H. 2011. AFM image processing for estimating the number and volume of nanoparticles on a rough surface. Surf Interface Anal 43:1354–1359.

Liu X, Luo T, Chen Y, Huang W, Piaszenski G. 2012. Optimal design and fabrication of three-dimensional calibration

specimens for scanning probe microscopy. Rev Sci Instrum 83:053708.

Lui CH, Liu L, Mak KF, Flynn GW, Heinz TF. 2009. Ultraflat graphene. Nature 462:339–341.

Manjón JV, Carbonell-Caballero J, Lull JJ, et al. 2008. MRI denoising using non-local means. Med Image Anal 12:514–523.

Nemes-Incze P, Osváth Z, Kamarás K, Biró LP. 2008. Anomalies in thickness measurements of graphene and few layer graphite crystals by tapping mode atomic froce microscopy. Carbon 46:1435–1442.

Orji NG, Dixson RG, Fu J, Vorburger TV. 2004. Traceable picometer level step height metrology. Wear 257:1264–1269.

Salmon J. 2010. On two parameters for denoising with non-local means. IEEE Signal Proc Let 17:269–272.

Shi Z, Yang R, Zhang L, et al. 2011. Patterning graphene with zigzag edges by self-aligned anisotropic etching. Adv Mater 23:3061–3065.

Thacker NA, Manjon JV, Bromiley PA. 2010. Statistical interpretation of non-local means. IET Comput Vis 4: 162–172.

Wang S, Xia Y, Liu Q, et al. 2012. Gabor feature based nonlocal means filter for textured image denoising. J Vis Commun Image R 23:1008–1018.

Wu Y, Tracey B, Natarajan P, Noonan JP. 2013. Probabilistic non-local means. IEEE Signal Proc Let 20:763–766.